Journal of Digital Imaging (2020) 33:1292–1300
https://doi.org/10.1007/s10278-020-00363-9

Four-Dimensional Cone-Beam Computed Tomography Image Compression Using Video Encoder for Radiotherapy

Hui Yan[1] · Yexiong Li[1] · Jianrong Dai[1]

Published online: 24 June 2020

Abstract
Four dimensional cone-beam computed tomography (4D-CBCT) images were widely used for patient positing and target localization in radiotherapy. As consisting of multiple CBCT sets, it needs more time and space for data transferring and storage. In this study the feasibility of applying video coding algorithms for 4D-CBCT image compression was investigated. Prior to compression 4D-CBCT images were arranged in an order based on breathing phase or slice location for input sequence of video encoder. Median filtering was applied to suppress noise and artifact of 4D-CBCT for improved image quality. Three popular video coding algorithms (Motion JPEG 2000, Motion JPEG AVI, and MPEG-4) were tested and their performances were evaluated on a publicly available 4D-CBCT database. The average compression ratio of MPEG-4 was 135, while the values of Motion JPEG AVI and Motion JPEG 2000 were 16 and 7, respectively. The compression rate of two ordering methods was comparable and the location-based ordering method was slightly higher. With pre-processing of median filtering, the inter-frame similarity of input sequence was improved and the resulting compression rate was increased. MPEG-4 provided extremely higher compression rate for 4D-CBCT images. The ordering method based on slice location resulted in higher compression rate than the ordering method based on breathing phase. The median filtering was effective in improving inter-frame similarity and resulted in higher compression rate. The video coding algorithms are not only applicable for 4D image modalities but also feasible for serial 3D image modalities.

Keywords 4D-CBCT · Video coding algorithm · Image compression

Introduction

4D-CBCT is an emerging imaging technique for monitoring organ motion of patient under radiotherapy. Internal organ motion caused by respiration or heartbeat is considerable. It is crucial to verify reproducibility of target location prior to treatment for lung and abdominal cancer patients [1–3]. Recently, the external and surface monitoring systems, such as RPM and OSMS (Varian Medical System, Palo Alto, USA), were used for patient positioning in radiotherapy. However they were not able to track the motion of internal target. Combining external surveillance signal with 4D-CBCT images was an effective way in monitoring real-time internal organ motion for high-precision treatment such as hypofraction radiotherapy or radiosurgery [4, 5].

In clinic, 4D-CBCT images were reconstructed from thousands of 2D X-ray projections acquired by an on-board kilovoltage imaging system while gantry rotates during multiple breathing cycles [6]. Comparing with fan-beam CT (FBCT) with high contrast-to-noise ratio, the geometry of cone-beam CT (CBCT) causes the photons to deviate from their original path and results in increased scatter artifact due to a larger field of view (FOV). Scatter is the primary factor in deteriorating CBCT image quality, such as cupping artifact, degradation of contrast, and enhancement of noise in CBCT images [7]. Apart from the scatter artifacts, 4D-CBCT may subject to the increased motion artifact due to the extended image acquisition time [8]. The moving structures cause blurring or streaking artifacts. It could be reduced by patient immobilization systems but never eliminated. In general, 4D-CBCT is more prone to motion artifact in addition to routine scatter artifacts.

The size of 4D-CBCT is usually larger since it consists of multiple phase CBCT sets. With increasing applications of

✉ Jianrong Dai
dai_jianrong@163.com

[1] Department of Radiation Oncology, National Cancer Center/ National Clinical Research Center for Cancer/Cancer Hospital, Chinese Academy of Medical Sciences and Peking Union Medical College, Beijing 100021, China

4D-CBCT in radiotherapy, data transferring and storage became a huge burden for routine clinical practice. For a lung cancer patient with daily 4D-CBCT scan (33 fractions, 3-mm slice thickness, and 10 breathing phases), the total size of 4D-CBCT images in the whole treatment courses would be approximately 8 GB. For a cancer center treated with 300 patients per day, if only 10% of patients were using 4D-CBCT scan, the total size of images would be 240 GB per day and approximately 5 TB per month. To transfer and backup such huge amount of 4D-CBCT data would be a challenge for a busy clinic.

Video coding was successfully applied to 4DCT images, and extremely high compression rate was achieved in our previous study [9]. We extended this application to 4D-CBCT images and expected the same high compression performance to be achieved. Three popular video encoders employing lossy intra-frame coding, lossless intra-frame coding, and lossy inter-frame coding algorithms were tested [10, 11]. Two ordering methods and median filtering were applied and their effectiveness was evaluated. In Section 2 the principles of image and video coding algorithms were introduced and followed by the explanation of two ordering methods and median filtering. In Section 3, the performance of video coding algorithms was examined on a publicly available database. The results with respect to the two ordering methods and median filtering were reported. Finally, the advantages and disadvantages of the method were discussed.

Materials and Methods

Inter-Frame Coding Algorithm

The traditional image compression methods focus on static image. It first calculates discrete cosine transform (DCT) or wavelet transform (WT) over image. The resulted coefficients is then quantized and coded to bit stream. Finally, the bit stream is saved to a file. For maximizing compression rate, the smaller coefficients are discarded during quantization which causes data loss. Accordingly, image compression can be categorized in lossless and lossy techniques. Lossless techniques are reversible and compression rates are low. Lossy techniques are irreversible and compression rates are much higher. The most popular compression algorithms in the medical image community are JPEG and JPEG 2000 [12, 13].

For serial images, such as movie clip consisting of motion frames, the traditional image compression techniques were not sufficient. Therefore, video coding techniques were quickly developed to explore spatial and temporal relationship between adjacent images for higher compression rate [14]. The inter-frame coding algorithm is the most effective one and was adopted by many famous international organizations such as Moving Picture Experts Group (MPEG) and Visual Coding Experts Group (VCEG) [15, 16]. Among inter-frame coding algorithms, MPEG-4 is the most used in multi-media recording and transferring. It employs advanced inter-frame prediction coding algorithm to provide extremely higher compression ratio for video generation.

The workflow of MPEG-4 video coding algorithm was shown in Fig. 1. The encoding process of MPEG-4 was illustrated at the top box of Fig. 1. First, the original image $f_n(x,y)$ at index n is compared with the reference image $r_n(x,y)$. $r_n(x,y)$ could be the original image $f_{n-1}(x,y)$ at index n-1 or the others depending on the types of coding algorithms. The similar areas between $f_n(x,y)$ and $r_n(x,y)$ are sought and the motion vector v(i,j) is calculated. Based on v(i,j), the image $\hat{f}_n(x,y)$ is predicted from $r_n(x,y)$ via motion compensator. The difference image $e_n(x,y)$ between $f_n(x,y)$ and $\hat{f}_n(x,y)$ is then calculated. Since $e_n(x,y)$ contains most of smaller values, it is more suitable for compression. Next, the different image $e_n(x,y)$ goes through regular image compression pipeline consisting of transform, quantization, and coding processes. The transform process converts $e_n(x,y)$ to coefficients via DCT or WT. The quantization process removes most of smaller coefficients. The coding processes assemble the coefficients together with motion vector to bit stream.

The decoding process of MPEG-4 was illustrated at the bottom box of Fig. 1. As the reverse process of encoder, the bit stream is first disassembled to coefficients and motion vector. These coefficients are then dequantized to regular transform coefficients. The difference image $e_n(x,y)$ is then recovered from these transform coefficients via inverse transform. Meanwhile, the image $\hat{f}_n(x,y)$ is predicted from the reference image $r_n(x,y)$ and motion vector v(i,j) via motion compensator. Finally, the original image $f_n(x,y)$ is recovered from the sum of $\hat{f}_n(x,y)$ and $e_n(x,y)$. Since only $e_n(x,y)$ and v(i,j) are saved in video file, the inter-frame coding algorithm usually results in a higher compression rate. Note that there could be minor information loss due to quantization process which removes the coefficients corresponding to high-frequency components and stores the coefficients corresponding to low-frequency components of the image [17, 18]. Since the human eye is sensitive to low-frequency feature of image, the loss of certain high-frequency components is visually indistinguishable.

Ordering Methods of Input Sequence

4D-CBCT image is usually reconstructed from X-ray projections corresponding to 10 breathing phases of 0%, 10%, …, 90% in a respiratory cycle. The 0% phase corresponds to the end of inhalation, and the 50% phase corresponds to the end of exhalation. During acquisition, the respiratory signal is acquired and used to sort the raw projection data into 10 breathing phases. The CBCT image is reconstructed from sorted projections and saves to a folder corresponding to the

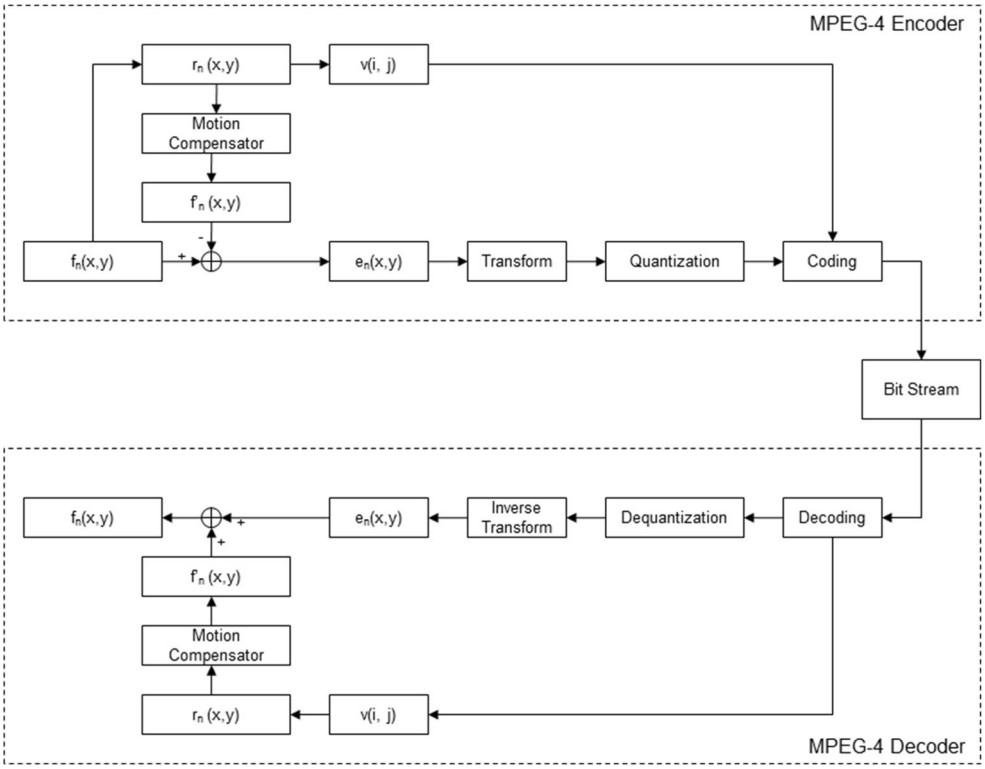

Fig. 1 The workflow of MPEG-4 video encoder and decoder. The top is encoding processing and the bottom is decoding process

breathing phase. Differed from 3D-CBCT, 4D-CBCT stores each phase CBCT in a separate folder. As a result, there are 10 sub-folders of phase CBCT images corresponding to 10 breathing phases in a 4D-CBCT folder.

The input of video coding algorithm is an image sequence arranged in given order. The ordering method determines the similarity between adjacent images of input sequence. Therefore, the ordering methods affect overall correlation quality of input sequence and subsequently compression rate of video encoder. Given this reason, the selection of ordering methods for input sequence of video encoder is important. Two ordering methods based on spatial and temporal relationship of 4D-CBCT images were investigated in this study.

The demonstration of the two ordering methods were shown in Fig. 2. The first ordering method is to line up all images in a CBCT subset by their slice locations and proceeds to next CBCT subset to line up all images in the same manner until all CBCT subsets are processed. The procedure to form a sequence in this way is shown Fig. 2a. The resulting sequence is a phase-prioritized (PP) sequence since the sequence is assembled based on phase set of CBCT images. The second ordering method is to line up all images at the same depth in all CBCT subsets and proceed to the next depth to line up all images in the same manner until all depths are processed. The procedure to form a sequence in this way is shown Fig. 2b. The resulting sequence is a location-prioritized (LP) sequence since the sequence is assembled based on location/depth of CBCT images. Note that the two ordering methods are simple in implementation and there would be more complex ordering methods to be explored.

Median Filtering for Noise Suppressing

Due to cone beam geometry and extended acquisition time, 4D-CBCT image suffers strong noise and artifacts. As an example, one 4D-CBCT image was shown in Fig. 3a. The top-left sub-plot is the histogram of intensity distribution of pixels. The right and bottom sub-plots are the profiles at middle lines of image. The noise and streak artifacts in original 4D-CBCT image are pronounced. For this reason, noise suppression is important to improve image quality and potentially correlation quality of input sequence.

Median filtering is an effective way to remove speckle and salt-and-pepper noise while preserving the edge information of original image. In this study, median filtering in two dimensions was applied. As shown in Figs. 3b–d, 4D-CBCT images after pre-processing of median filtering with different neighborhood sizes were demonstrated. After processing of median filtering, the noise level is reduced and the edge characteristic is well maintained. Note that if larger neighborhood size was used, the edge information of image would be blurred. In this study, three small neighborhood sizes (2×2, 3×3, 4×4) were used and their effects on compression performance were evaluated.

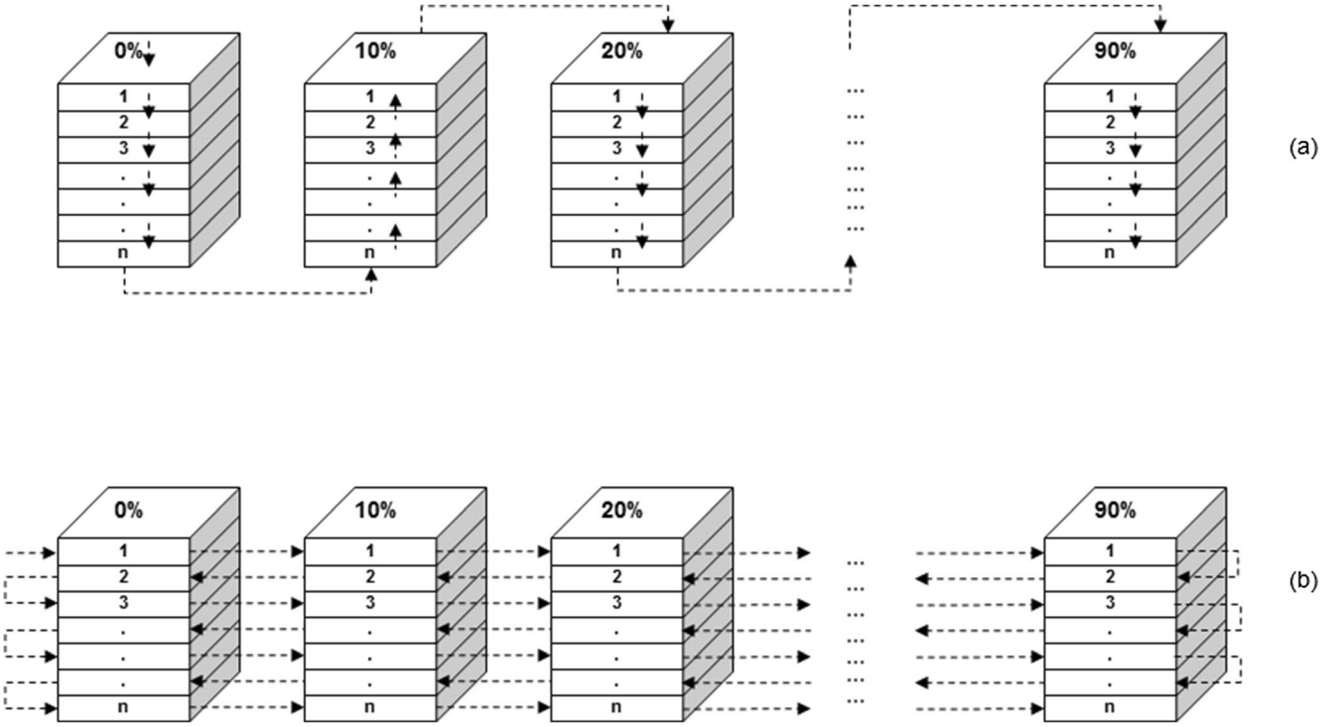

Fig. 2 The illustration of (**a**) phase-prioritized ordering method and (**b**) location-prioritized ordering method. 0%, 10%, …, 90% are 10 stacks of phase CBCT sets. 1, 2, …, *n* are slices indexes of phase CBCT set. The arrow indicates the direction of the next image in input sequence

Clinical Evaluation

The collection of 4D-Lung dataset was downloaded from the TCIA website and used for testing. This dataset consists of 507 4D-CBCT images in a population of 20 locally advanced non-small cell lung cancer patients under treatment of radiotherapy [8]. Daily 4D-CBCT images were acquired on a commercial onboard CBCT scanner. Approximately 2000–2500 projections were acquired over a period of 8–10 min in half-fan mode with half bow-tie filter. The technique was 125 kVp, 20 mA, and 20 ms in a single 360 slow gantry arc. Using the external surrogate, the CBCT projections were sorted into 10 breathing phases and reconstructed with an in-house FDK reconstruction algorithm. The total size of the 4D-CBCT dataset is 126 GB and 20% of them were used for testing. As an example, for a patient with 20 treatment fractions of radiotherapy, the 4D-CBCT datasets acquired at days 1, 5, 10 15, and 20 were selected. Three video coding algorithms were investigated in this study. They are Motion JPEG 2000 (MJ2) which is lossless and intra-frame coding algorithm, Motion JPEG AVI (AVI) which is a lossy and intra-frame coding algorithm, and MPEG-4 (MP4) which is a lossy and inter-frame coding algorithm. The coding algorithms were implemented by Matlab functions (MathWorks, Inc. Natick, MA). All tests were performed on a Dell Precision Tower 5810 personal computer equipped with Intel i7 CPU 2.4-GHz and 72 GB RAM.

The compression performance of video encoders is quantified by compression time and compression ratio (CR). Compression time is the average time on processing one 4D-CBCT image which includes the time expending on median filtering and encoding. Compression ratio is the ratio between the sizes of 4D-CBCT images and video file generated by video encoder. The overall correlation quality of a sequence is quantified by mean inter-frame difference (MIFD) and mean inter-frame correlation coefficient (MIFCC). MIFD is calculated by the mean value of differences between all pairs of adjacent images of input sequence, while MIFCC is calculated by the mean value of correlation coefficients between all pairs of adjacent images of input sequence. The information loss due to compression is quantified by two metrics, mean square error (MSE) and peak signal-to-noise ratio (PSNR) [19]. The MSE is calculated by comparing original and decompressed images pixel by pixel. PSNR is the ratio between the maximum power of a signal and the power of corrupting noise that affects the fidelity of its representation. Here, MAX is the maximum possible pixel value of the image and 2^{16}–1 in this study. Typical values for the PSNR of lossy image and video compression are between 60 and 80 dB, provided the bit depth is 16 bits.

Results

Video Encoders

The performance of three video coding algorithms with respect to two ordering methods was summarized in Table 1. The

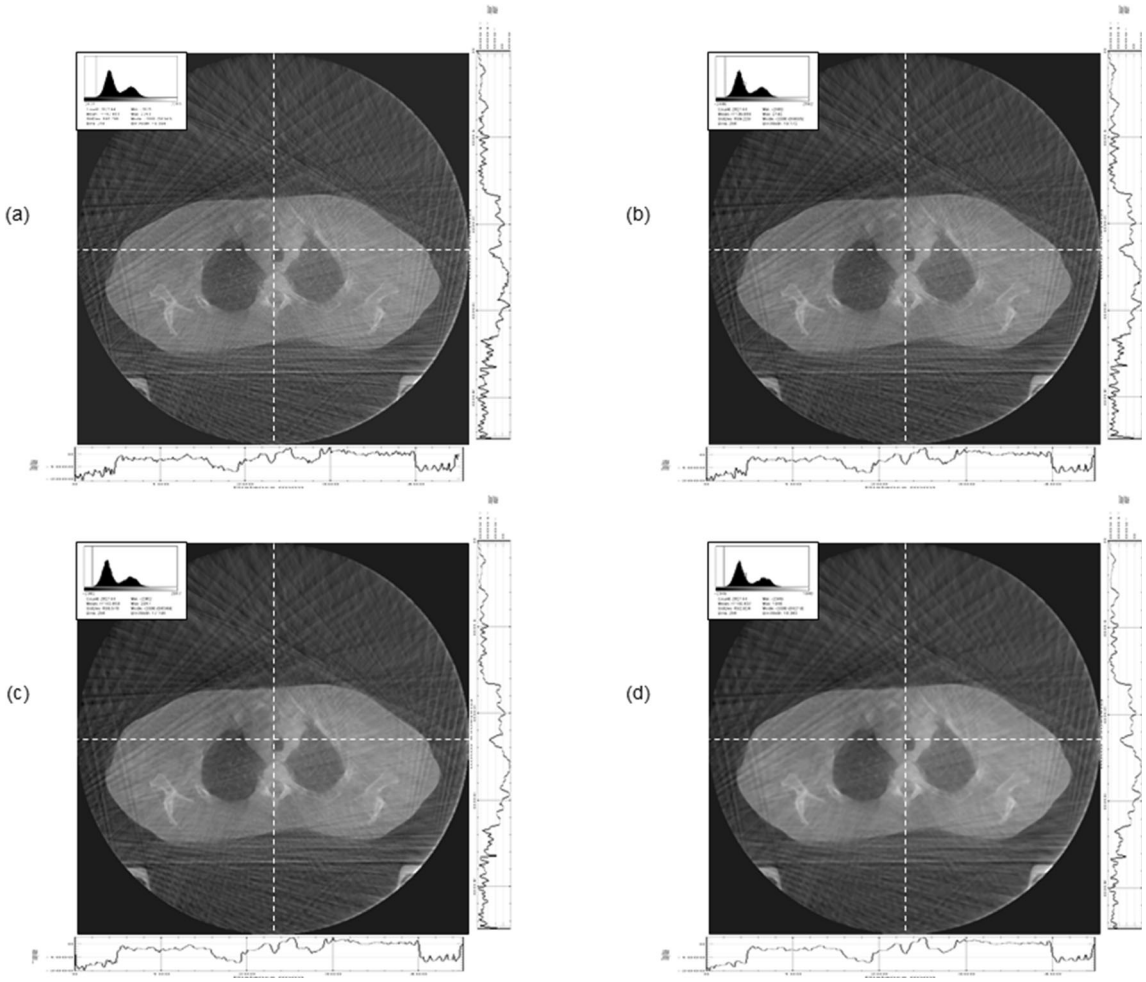

Fig. 3 Example of 4D-CBCT image processed by median filtering with neighborhood size (**a**) 1 × 1, (**b**) 2 × 2, (**c**) 3 × 3, (**d**) 4 × 4. The sub-plot at top-left corner is the histogram of intensity distribution of pixels. The sub-plots at right and bottom sides are profiles along vertical and horizontal axes. The locations of profiles at middle lines are represented by white dot lines in each figure

compression time of MJ2 and AVI are 13.7 ms and 23.4 ms, respectively. The compression time of AVI is more because its coding algorithm is more complex. Note that since MJ2 and AVI are static image-based coding algorithms, the compression time for both ordering methods is identical. The compression time of MP4 are 26.2 ms and 13.1 ms for phase-prioritized and location-prioritized ordering methods, respectively. The compression time of phase-prioritized ordering method is more than that of location-prioritized ordering method.

The compression ratio of MJ2 and AVI are 7.2 ± 0.8 and 16.4 ± 7.1, respectively. The compression ratio of AVI is higher than that of MJ2 since AVI is a lossy coding algorithm. Note that since MJ2 and AVI are static image-based coding algorithms, the compression ratios for both ordering methods are identical. The compression ratios of MP4 are 135.2 ± 92.9 and 137.9 ± 100.4 for phase-prioritized and location-prioritized ordering methods, respectively. The compression ratio of location-prioritized ordering method is higher than that of phase-prioritized ordering method. The compression ratio of MP4 is the highest one among three video encoders.

There is no data loss of MJ2 since it is a lossless coding algorithm. For AVI, the values of MSE and PSNR are 0.017

Table 1 Performance of three video encoders with respect to two ordering methods for 4D-CBCT compression

Ordering	Similarity Metrics	MJ2f				AVI			MP4f			
	MIFD	MIFCC	T	CR	T	CR	MSE	PSNR	T	CR	MSE	PSNR
Phase-prioritized	89.8 ± 25.7	0.98 ± 0.0	13.7	7.2 ± 0.8	23.4	16.4 ± 7.1	0.017	66.7	26.2	135.2 ± 92.9	0.036	64.5
Location-prioritized	92.5 ± 31.3	0.98 ± 0.0	13.7	7.2 ± 0.8	23.4	16.4 ± 7.1	0.017	66.7	13.1	137.9 ± 100.4	0.035	64.6

and 66.7, respectively. Note that since AVI is a static image-based coding algorithm, its values of MSE (or PSNR) for both ordering methods are identical. For MP4, the values of MSE and PSNR are 0.036 and 64.5 for phase-prioritized ordering method, while they are 0.035 and 64.6 for location-prioritized ordering method. The values of MSE and PSNR of MP4 for both ordering methods are nearly identical.

Ordering Methods

The mean values of MIFD and MIFCC are 89.8 ± 30.3 and 0.98 ± 0.02 for phase-prioritized ordering method, while they are 92.5 ± 11.2 and 0.98 ± 0.01 for location-prioritized ordering method. The difference of MIFDs (ΔMIFD) between location-prioritized and phase-prioritized methods was calculated by $MIFD_{LP}$-$MIFD_{PP}$. Here, the subscripts LP and PP are abbreviations of location-prioritized and phase-prioritized methods, respectively. The histogram of ΔMIFD for all datasets was plotted as shown in Fig. 4a. Similarly, the difference of MIFCCs (ΔMIFCC) between two ordering methods was calculated by $MICC_{LP}$-$MIFCC_{PP}$, and the difference of CR (ΔCR) between two ordering methods was calculated by CR_{LP}-CR_{PP}. The histograms of ΔMIFCC and ΔCR for all tested datasets were shown in Fig. 4b and c, respectively.

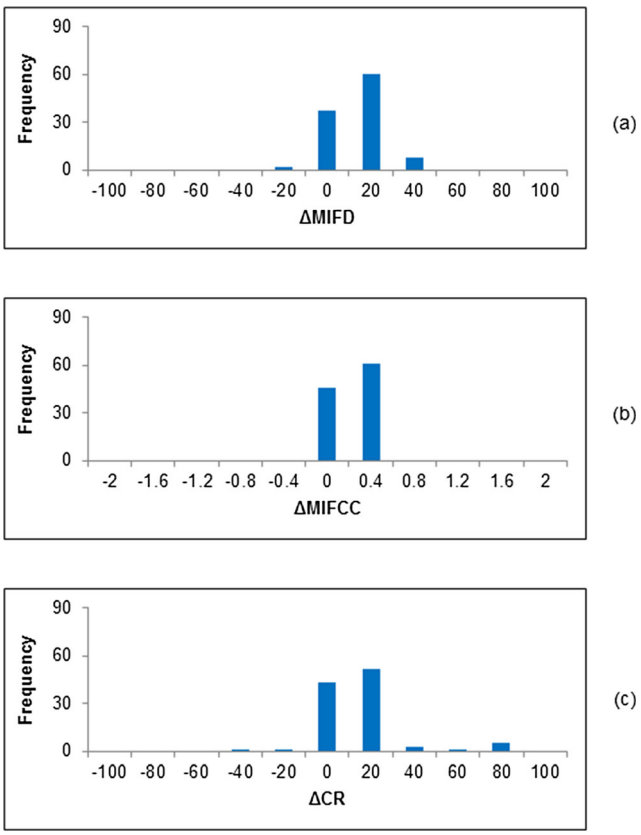

Fig. 4 The histograms of (**a**) ΔMIFD, (**b**)ΔMIFCC, and (**c**) ΔCR for all tested datasets

Note that the values of ΔMIFCC were scaled by a factor of 100. For most of tested datasets, MIFD, MIFCC, and CR of location-prioritized ordering method are more than that of phase-prioritized ordering method.

To illustrate the correlation relationship between similarity metrics and compression ratio of video encoder, the scatter plots of MIFD versus CR and MIFCC versus CR were plotted in Fig. 5a and b. The data points belonging to the location-prioritized and phase-prioritized ordering methods were labeled by red plus and blue minus. And the trend lines were created for both ordering methods. As shown in Fig. 5, for both ordering methods, CR is inversely linear correlated with MIFD and linear correlated with MIFCC.

Median Filtering

The effect of neighborhood size of median filtering on compression performance of video encoders was summarized in Table 2. As the neighborhood size increased, MIFD is decreased and MIFCC is constant for both ordering methods. As the neighborhood size increased, the compression ratios of video are slightly increased for both ordering methods. MSE and PSNR are decreased as neighborhood size increased for both ordering methods. Overall, the improvement of similarity metric and compression ratio are in proportion to the

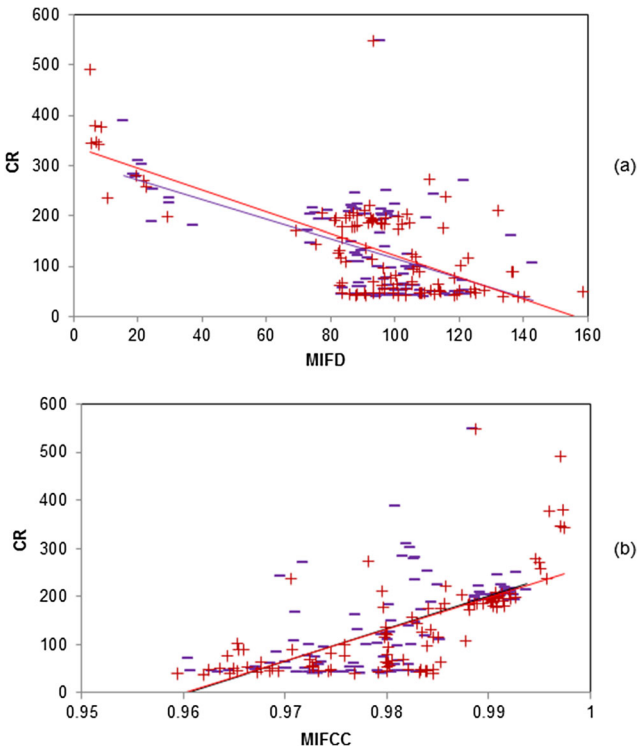

Fig. 5 The scatter plots of (**a**) MIFD vs. CR and (**b**) MIFCC vs. CR of MP4. The points resulted by location-prioritized and phase-prioritized ordering methods were labeled by red plus and blue minus. Their trend lines were shown in red and blue color, respectively

Table 2 Compression performance of three video encoders with respect to four neighborhood sizes of median filtering

Size	Phase-prioritized						Location-prioritize					
	MIFD	MIFCC	T	CR	MSE	PSNR	MIFD	MIFCC	T	CR	MSE	PSNR
1 × 1	89.8 ± 25.7	0.98 ± 0.0	26.2	135.2 ± 92.9	0.036	64.5	92.5 ± 31.3	0.98 ± 0.0	13.1	137.9 ± 100.4	0.035	64.6
2 × 2	75.8 ± 21.3	0.98 ± 0.0	26.3	135.1 ± 94.6	0.049	63.0	76.6 ± 26.5	0.98 ± 0.0	13.2	140.2 ± 102.6	0.047	63.1
3 × 3	67.2 ± 19.7	0.98 ± 0.0	26.3	141.4 ± 99.4	0.057	62.3	66.9 ± 24.5	0.98 ± 0.0	13.0	145.5 ± 109.2	0.056	62.5
4 × 4	57.0 ± 16.2	0.98 ± 0.0	26.7	143.6 ± 96.3	0.073	61.1	55.5 ± 20.5	0.98 ± 0.0	13.1	148.2 ± 104.9	0.073	61.2

increase of neighborhood size of median filtering. The decrease of information loss is in proportion to the decrease of neighborhood size of median filtering.

The histograms of ΔMIFD, ΔMIFCC, and ΔCR with respect to the different neighborhood sizes of median filtering were shown in Fig. 6. While comparing Fig. 6a, d, and g, the majority of ΔMIFD is decreased as the neighborhood size increased. The location-prioritized ordering method mostly results in larger value of MIFD. While comparing Fig. 6b, e, and h, the majority of ΔMIFCC are slightly increased as the neighborhood size increased. The location-prioritized ordering method mostly results in larger value of MIFCC. While comparing Fig. 6c, f, and i, the majority of ΔCR are slightly increased as the neighborhood size increased. The location-prioritized ordering method mostly results in larger value of CR.

To evaluate the effect of median filtering on compression ratio, the scatter plots of MIFD vs. CR and MIFCC vs. CR were plotted in Fig. 7 with respect to the three neighborhood sizes of median filtering. The data points belonging to location-prioritized and phase-prioritized ordering methods

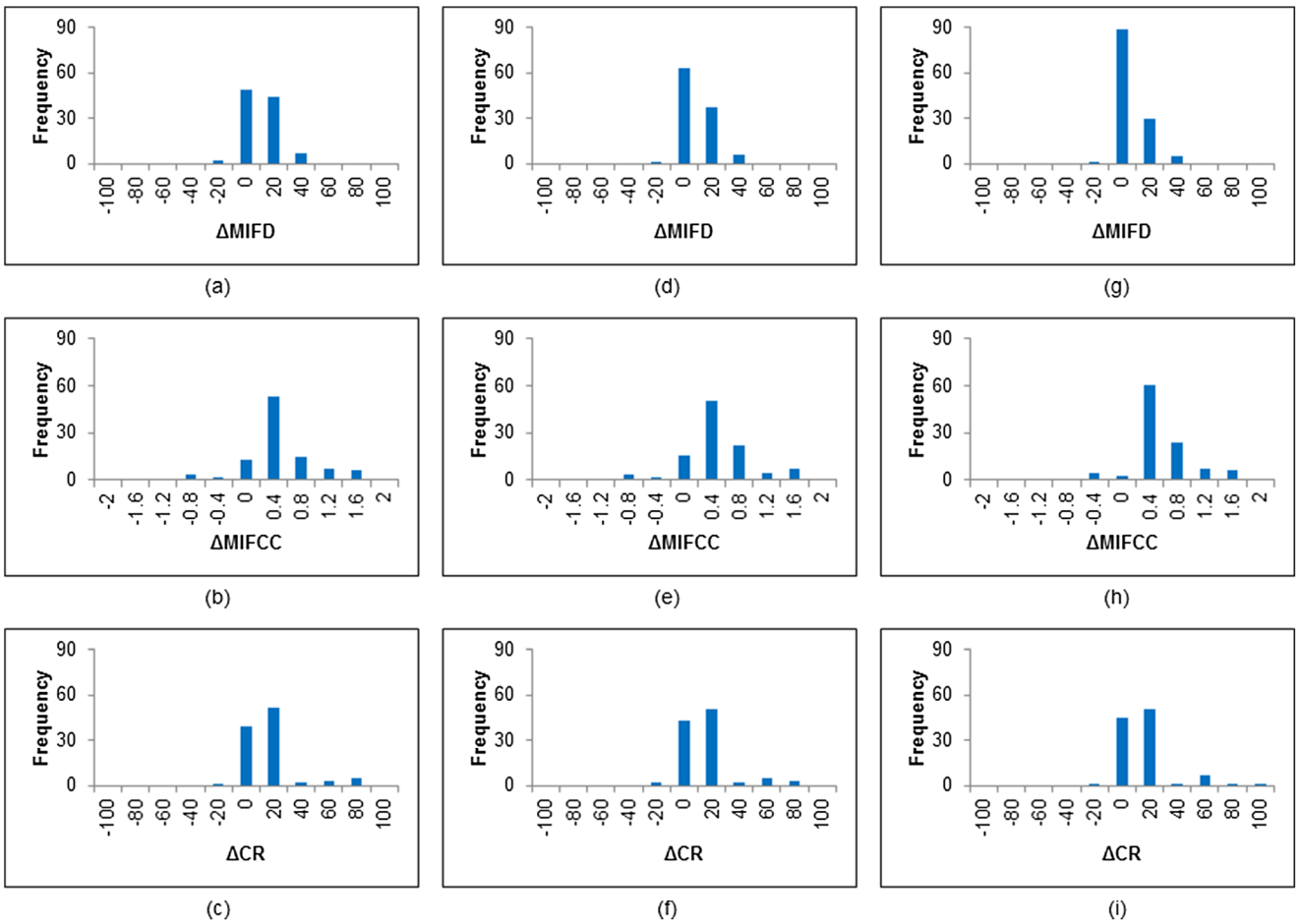

Fig. 6 The histograms of (**a**) ΔMIFD, (**b**)ΔMIFCC, and (**c**) ΔCR for neighborhood size (2 × 2) of median filtering. The histograms of (**d**) ΔMIFD, (**e**) ΔMIFCC, and (**f**) ΔCR for neighborhood size (3 × 3) of median filtering. The histograms of (**g**) ΔMIFD, (**h**) ΔMIFCC, and (**i**) ΔCR for neighborhood size (4 × 4) of median filtering

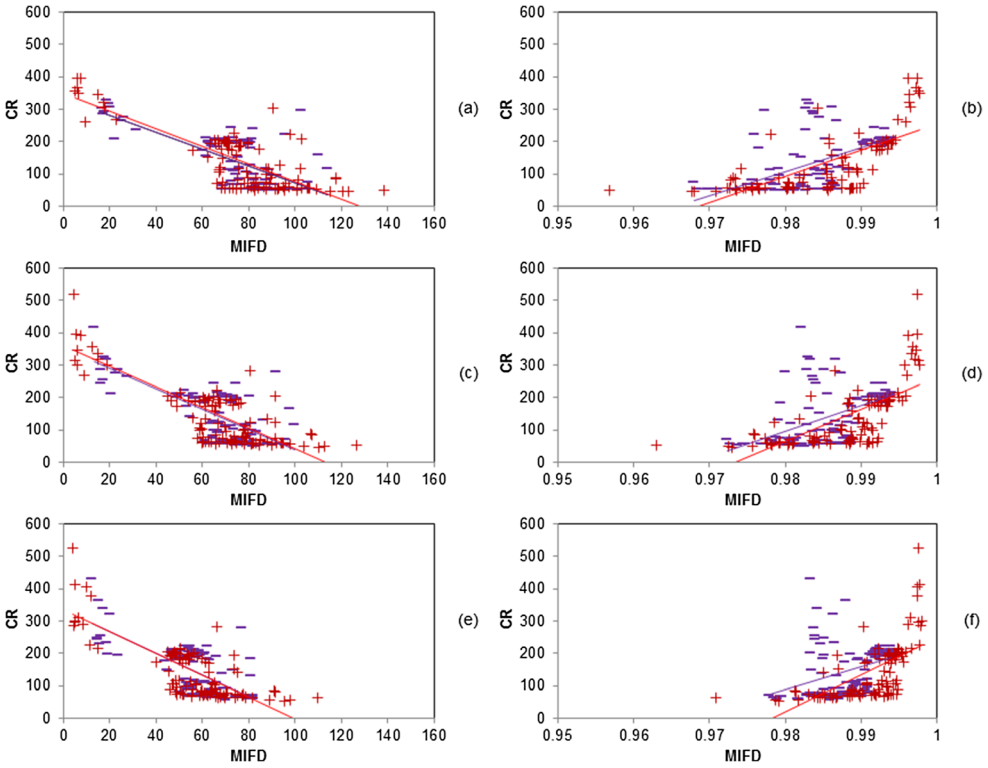

Fig. 7 The scatter plots of (**a**) MIFD vs. CR and (**b**) MIFCC vs. CR for neighborhood size (2 × 2) of median filtering. The scatter plots of (**c**) MIFD vs. CR and (**d**) MIFCC vs. CR for neighborhood size (3 × 3) of median filtering. The scatter plots of (**e**) MIFD vs. CR and (**f**) MIFCC vs. CR for neighborhood size (4 × 4) of median filtering. The data points resulted by location-prioritized and phase-prioritized ordering methods were labeled by red plus and blue minus. Their trend lines were shown in red and blue colors, respectively

were represented by red plus and blue minus. And the trend lines were created for both ordering methods. While comparing among Fig. 7a, c, and e, the mean value of MIFD is decreased as the neighborhood size increased. The gap between trend lines of the two ordering methods becomes smaller as the neighborhood size increased. While comparing among Fig. 7b, d, and f, MIFCC is increased as neighborhood size increased. The gap between trend lines of the two ordering methods becomes larger while the neighborhood size increased.

Discussions

MP4 demonstrated its superior compression performance over AVI and MJ2. This is because MP4 utilizes correlation information between adjacent images of input sequence and maximally reduces redundancy within 4D-CBCT images. Both ordering methods demonstrated excellent compression performance. The location-prioritized ordering method was slightly better as the similarity of its input sequence is higher. The similarity metrics, MIFD and MIFCC, correlated with compression ratio well for most of the tested datasets. This implied that improving inter-frame similarity of input sequence could potentially increase compression ratio of MP4 or the other inter-frame coding algorithms. The noise and artifact of 4D-CBCT images were higher comparing with those of 4DCT images. With pre-processing of median filtering, the inter-frame similarity of input sequence were improved and subsequently resulted in higher compression ratio.

Data loss due to image compression was investigated in this study. It may cause certain degrees of image deterioration and is varied by video coding algorithms. As shown in Table 1, the data loss caused by MP4 is less than that by AVI according to the metrics of MSE and PSNR. For all tested datasets in Table 1, MSE is less than 0.05 and PSNR is within 60–65 by MP4. This indicated that the majority of 4D-CBCT image content is well preserved and the data loss due to quantization process is less. The median filtering may cause certain degrees of blurring effect. However, the edge information of 4D-CBCT images was well preserved. As shown in Table 2, for different neighborhood sizes of median filtering, the values of MSE and PSNR are changed slightly. This indicated that the influence of blurring effect caused by median filtering on 4D-CBCT images is less. It should note that current MP4 encoder is based on H.264 standard and will be substituted by H.265 standard which provides substantially improved video quality at the same bit rate.

So far there were few medical applications adopting lossy image compression methods. This is because of the regulatory policies required by many agencies and governments. Given the fact that CBCT was designed for patient positioning, the lossy video encoder such as MP4 might be acceptable for clinical use [20]. This will save lots of time and space for hospitals. For example, a 126GB 4D-CBCT dataset can be compressed to a 0.9GB file by MP4. In other words, it will save 99%

transferring time and disk space for this 4D-CBCT dataset. In addition to higher compression ratio provided by MP4, the compressed file can be easily played by most of commercial or free media players, such as Windows media player. It is unnecessary to decompress a video file before watching its content. This feature would be very suitable for many web-based and cloud-based medical image applications.

The implementation of this method in clinic is similar to those commonly used compression software, such as Winzip (WinZip International LLC, Mansfield, Connecticut). We developed a stand-alone executable program based on Matlab application deployment strategy (The MathWorks, Inc., Natick, MA). For image compression, the user only needs to select one folder to locate 4D-CBCT images and another folder to save a video file. This program then proceeds to compress 4D-CBCT images into a single video file. For image decompression, the user only needs to select one folder to locate video file and another folder to save decompressed images. This program then proceeds to decompress a video file into 4D-CBCT images and saved 10 phase CBCT sets in 10 subfolders, respectively. It should note that besides compression of 4D-CBCT images, this method is also applicable to the other 4D image modalities and serial 3D image modalities.

Conclusion

Comparing with MJ2 and AVI, MP4 could provide extremely high compression rate for 4D-CBCT image. With properly selected ordering method and pre-processing of median filtering, the compression rate of MP4 could be further improved. The application of MP4 for 4D-CBCT image compression could save lots of clinical time and space for data transferring and storage. This method is not only applicable for most of 4D image modalities but also feasible for those serial 3D image modalities.

Funding Information This work was partially supported by National Key R&D Program of China (2016YFC0904600) and China National Science Foundation (CNSF11875320).

Compliance with Ethical Standards

Conflict of Interest The authors declare that they have no relevant conflict of interest.

References

1. Korreman SS: Image-guided radiotherapy and motion management in lung cancer. Br J Radiol 88(1051):20150100,2015.
2. Kwong Y, Mel AO, Wheeler G, Troupis JM: Four-dimensional computed tomography (4DCT): A review of the current status and applications.J Med Imaging Radiat Oncol 59(5):545-54,2015.
3. Moorrees J, Bezak E: Four dimensional radiotherapy: a review of current technologies and modalities. Australas Phys Eng Sci Med 35(4):399-406,2012.
4. Keall P: 4-dimensional computed tomography imaging and treatment planning.Semin Radiat Oncol 14(1):81-90,2004.
5. Panta RK, Segars P, Yin FF, Cai J: Establishing a framework to implement 4D XCAT phantom for 4D radiotherapy research. J Cancer Res Ther 8(4):565-70,2012.
6. Hugo GD, Weiss E, Sleeman WC, Balik S, Keall PJ, Lu J, Williamson JF: A longitudinal four-dimensional computed tomography and cone beam computed tomography dataset for image-guided radiation therapy research in lung cancer. Med Phys 44(2):762-771,2017.
7. Posiewnik M, Piotrowski T: A review of cone-beam CT applications for adaptive radiotherapy of prostate cancer. Phys Med 59:13-21,2019.
8. Srinivasan K, Mohammadi M, Shepherd J: Applications of linac-mounted kilovoltage Cone-beam Computed Tomography in modern radiation therapy: A review. Pol J Radiol 79:181-93,2014.
9. Yan H, Li Y, Dai J: Exploring Correlation Information for Image Compression of Four-Dimensional Computed Tomography. Quant Imaging Med Surg,2019. https://doi.org/10.21037/qims.2019.06.19
10. Noreña T, Romero E: Medical image compression: a review. Biomedica 33(1):137-51,2013.
11. Braunschweig R, Kaden I, Schwarzer J, Sprengel C, Klose K: Image data compression in diagnostic imaging: international literature review and workflow recommendation. Rofo 181(7):629-36, 2009.
12. Miaou SG, Ke FS, Chen SC: A lossless compression method for medical image sequences using JPEG-LS and interframe coding. IEEE Trans Inf Technol Biomed 13(5):818-21,2009.
13. Brennecke R, Bürgel U, Rippin G, Post F, Rupprecht HJ, Meyer J: Comparison of image compression viability for lossy and lossless JPEG and Wavelet data reduction in coronary angiography. Int J Card Imaging 17(1):1-12,2001.
14. Xu R, Pattanaik SN, Hughes CE: High-dynamic-range still-image encoding in JPEG 2000. IEEE Comput Graph Appl 25(6):57-64, 2005.
15. Bjontegaard G, Lillevold KO, Danielsen R: A comparison of different coding formats for digital coding of video using MPEG-2. IEEE Trans Image Process 5(8):1271-6,1996.
16. Lan C, Shi G, Wu F: Compress compound images in H.264/MPGE-4 AVC by exploiting spatial correlation. IEEE Trans Image Process 19(4):946-57,2010.
17. Fidler A, Skaleric U, Likar B: The impact of image information on compressibility and degradation in medical image compression. Med Phys 33:2832–2838,2006.
18. Fidler A, Skaleric U, Likar B: The effect of image content on detail preservation and file size reduction in lossy compression. Dentomaxillofac Radiol 36:387–392,2007.
19. Frankewitsch T, Söhnlein S, Müller M, Prokosch HU: Computed Quality Assessment of MPEG4-compressed DICOM Video Data. Stud Health Technol Inform 116:447-52,2005.
20. Koff DA, Shulman H: An overview of digital compression of medical images: can we use lossy image compression in radiology? Can Assoc Radiol J 57:211–217,2006.